ACS OMEGA

http://pubs.acs.org/journal/acsodf

Article

Highly Sensitive Surface-Enhanced Raman spectroscopy for the Surface Corrosion Analysis of Bronze Relics Using the Polyacrylonitrile/Polyvinylpyrrolidone Silver Nanoparticle Flexible Substrate

Pengyang Li, Yahui Zhang, Xia Huang,* Junying Chen, Jiachang Chen, Lei Li, and Xiaoqi Xi

Cite This: *ACS Omega* 2023, 8, 3091−3101

Read Online

ACCESS | Metrics & More | Article Recommendations

ABSTRACT: Surface-enhanced Raman spectroscopy (SERS) is widely used in biological and chemical analyses and in other fields because of its advantages such as high sensitivity and nondestructive nature. Ancient bronze cultural relics of China are exquisitely shaped and highly ornamental. Harmful rust components on the surface of bronze cultural relics have been extensively analyzed. SERS is beneficial to the surface composition analysis of ancient Chinese bronze relics and can be used for accurate characterization with almost zero damage to the surface. In this study, we designed a solution with polyacrylonitrile (PAN) and polyvinylpyrrolidone (PVP) macromolecules as precursors, which were electrospun and used as the nanofiber substrate. After tannic acid modification, the substrate was loaded with silver nanoparticles by using Tollens' reagent as the silver source and glutaraldehyde as the reducing agent in a water bath. The morphology and size of silver nanoparticles were adjusted by changing the reaction times. The effects of tannic acid and PVP as stabilizers were investigated. R6G and basic copper chloride were used as probe molecules for substrate SERS, and the Raman enhancement factor was calculated. The SERS performance of the substrate with high sensitivity was verified through characterization.

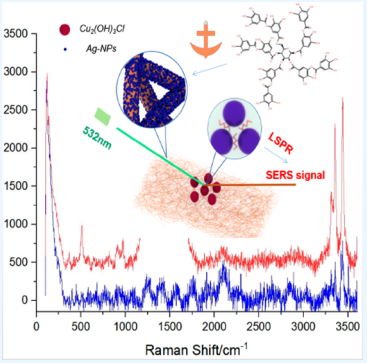

1. INTRODUCTION

Chinese bronze relics, which mark the development level of the slave social productive force of China, signify the wisdom of the ancient Chinese working people. These bronze relics show exquisite shapes, are unique in workmanship, and possess a high artistic value. They have a long history and have remained buried underground for thousands of years. To appreciate the elegant demeanor of ancient Chinese culture, protecting bronze relics has been a key project of China, and efforts have been made to prevent further corrosion of the bronze cultural relics. Analyzing the surface composition of the bronze relics has become crucial, but the ornamental significance of these relics limits the application of many detection and characterization methods. Their surface composition is complex, and dark green chlorite [$Cu_2(OH)_3Cl$], light green hydroxylchlorite [$CuCl_2{\cdot}3Cu(OH)_2$], and white chlorite [CuCl] available in basic copper chloride can accelerate the corrosion of the bronze relics.[1,2] For a long time, detection analyses have been performed through sampling; thus, studies are limited to cultural relic fragments.[3]

Surface-enhanced Raman spectroscopy (SERS) offers advantages, such as high sensitivity, no sample destruction, high precision, high repeatability, and fast output signal. SERS is widely used in various fields, including environmental monitoring, biological diagnosis, biological instruments, and chemical analyses. SERS is suitable not only for analyzing the surface composition of the bronze cultural relics but also for accurately and intuitively analyzing surface elements.[4,5] SERS is employed to detect and analyze targets by synthesizing nanostructure materials with SERS benefits and by using them as substrates. Many scholars have reported that the SERS effect mainly involves electromagnetic and chemical enhancement.[6] Electromagnetic enhancement occurs when a metal with rough surface is irradiated by light. Then, its plasma energy is excited to a higher energy level, and resonance occurs after coupling with the electric field; thus, electric field on the metal surface is enhanced, and the Raman signal of the detected substance is indirectly amplified. Chemical enhancement results from Raman signal amplification after charge

Received: October 3, 2022
Accepted: December 2, 2022
Published: January 10, 2023

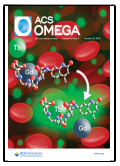

transfer between the substrate surface with SERS benefits and the detected substance.

In SERS, the hot spot is the key to obtain high sensitivity. The shape, spacing, and number of nanomaterials determine the hot spot of the SERS substrate. Ag is cheaper than Au and Pt. Ag has better stability than Cu; thus, Ag has been studied extensively.[7] Currently, solution and sputtering methods are mainly utilized for nanomaterial synthesis. Although nano-SERS substrates can be easily prepared by employing sputtering methods, this method is inconvenient—it is both expensive and time consuming. The solution method uses simple materials and is convenient for substrate preparation. Thus, it is suitable for synthesizing SERS substrates of various nanostructures.[8]

Electrospinning is a simple and easy method based on the principle of charging the droplets of extruder spinners. Electrostatic repulsion between the same surface charges gradually deforms the droplets into a Taylor cone and then turns them into a fiber state after they are stretched. This method involves the use of a flexible substrate to load the SERS substrate.

In this study, Ag nanoparticles with adjustable loading density were successfully prepared on polyacrylonitrile (PAN)/polyvinylpyrrolidone (PVP) composite nanofibers by employing the dip coating method. First, a PAN/PVP composite nanofiber mat was prepared through electrospinning. Then, the composite nanofiber mat was modified using tannic acid and immersed in Tollens' reagent to adsorb silver ammonia ions on the nanofiber surface. The silver nanoparticles were then grown on the PAN/PVP composite nanofiber mat through the glutaraldehyde reaction with Tollens' reagent. The results show that the loading and size of Ag nanoparticles can be controlled by adjusting the frequency of impregnation and reduction.

The morphology and structure of the PAN/PVP silver nanofiber mat were studied through field-emission scanning electron microscopy (SEM), transmission electron microscopy (TEM), and X-ray diffraction (XRD). The interaction modes of the nanofiber mat with silver nanoparticles and measured molecules were analyzed through infrared spectroscopy and thermal analyses. XRD was conducted to characterize the crystal state of the nanofiber mat. The SERS signals of rhodamine 6G (R6G) were used as the target molecule to evaluate the SERS activity, and the basic copper chloride powder was employed as the target molecule to analyze and simulate the surface elements of bronze ware. According to detection and characterization results, the prepared PAN/PVP silver nanofiber mat showed high SERS sensitivity and played a crucial role in the detection and analysis of the surface elements of the bronze cultural relics.

A single molecule of R6G has an obvious fingerprint region in the Raman spectrum, and it is one of the commonly used materials for the evaluation of Raman signal strength;[32,33,39] almost no obvious characteristic peak can be observed within 10^{-4} M, which helps distinguish the performance of SERS materials. Therefore, R6G was used in this experiment to further verify the SERS materials used in this study. Unearthed bronze cultural relics have a complex surface rust composition, but the rust, which can constantly erode the bronze cultural relics itself, is mainly the basic copper chloride [$Cu_2(OH)_3Cl$].[32,33] To protect bronze cultural relics, researchers have been dedicating their efforts to removing the harmful rust composition from the surface by using scientific methods. Therefore, selecting a suitable surface analysis technique is crucial. This study focuses on the second stage of the process of removal of harmful rust components from the surface to evaluate the function of the derusting material. Yet, only a few studies have used SERS, a nondestructive and highly sensitive trace representation technology, to detect harmful rust on the surface of bronze cultural relics. Therefore, the present study has pioneering significance for the protection of bronze cultural relics.

2. MATERIALS AND METHODS

2.1. Chemicals. Polyacrylonitrile (PAN; average molecular weight 85,000), polyvinylpyrrolidone (PVP; average molecular weight 58,000), silver nitrate standard solution, ammonia, *N*, *N*-dimethylformamide (DMF), tannins, rhodamine 6G, and glutaraldehyde were obtained from Maclean Chemical Reagents. The basic copper chloride powder was provided by Henan Cultural Relics Protection Center, Zhongyuan District, Zhengzhou City, Henan Province. All the chemicals were used as received without further purification.

2.1.1. Characterization. The nanofiber mat is spun using an electrospinning machine (Yunfan Technology DP30). The morphology of nanofibers and loaded silver nanoparticles was determined using a scanning electron microscope (Hitachi SU8010) and a field-emission electron microscope (Tecnai G2 F30 S-Twin transmission electron microscope). A 7 nm layer of gold was coated on the sample surface before SEM measurement. TEM samples were prepared using the nanomaterial; the nanomaterial was sonicated and dispersed in deionized water. The surface-enhanced Raman scattering for the samples was studied using a laser microscope and confocal Raman spectrometer (Renissau inVia). The crystallization status and composition of nanofiber mat surfaces were analyzed using an X-ray diffractometer (Panako bench X-ray diffractometer), a synchronous thermal analyzer (Naechi STA449F5), and an infrared spectrometer (Nicolet IS 10). All these experiments were conducted at a room temperature of 25 °C and a relative humidity of 45%.

2.2. Materials Preparation. *2.2.1. Preparation of the PAN/PVP Nanofiber Mat.* First, 1.4 g of PAN was added to 20 mL of DMF, followed by stirring for 6 h in a water bath at a constant temperature of 60 °C and under magnetic force. After homogenization of the solvent and PAN, a light yellow transparent solution was obtained. The solution was then removed and cooled to room temperature. Then, 0.6 g PVP was added to the cooled solution at one time, and the PAN/PVP spinning solution was prepared by stirring continuously for 1 h at room temperature until complete mixing. Before spinning, the spinning fluid was drawn into a 5 mL disposable plastic syringe with a 19 gauge steel needle, and the high-voltage electric field between the collection plate and metal tip showed a voltage of 16 kV. The injection speed of the polymer solution was 0.0008 mm/s, and the distance between the tip and collector was 10 cm. Finally, the nanofiber felt was collected on a grounded aluminum foil electrode plate, and the prepared nanofiber felt was carefully torn off from the aluminum foil and dried in an oven for 24 h for further processing.

To explore the relationship between PVP, the stabilizer, and the dispersant of silver nanoparticles, the PAN nanofiber mat was prepared using the following steps: 1 g of PAN was added to 10 mL of DMF, and the solution was stirred for 6 h in a water bath at 60 °C under magnetic force. After homogenizing

https://doi.org/10.1021/acsomega.2c06376
ACS Omega 2023, 8, 3091−3101

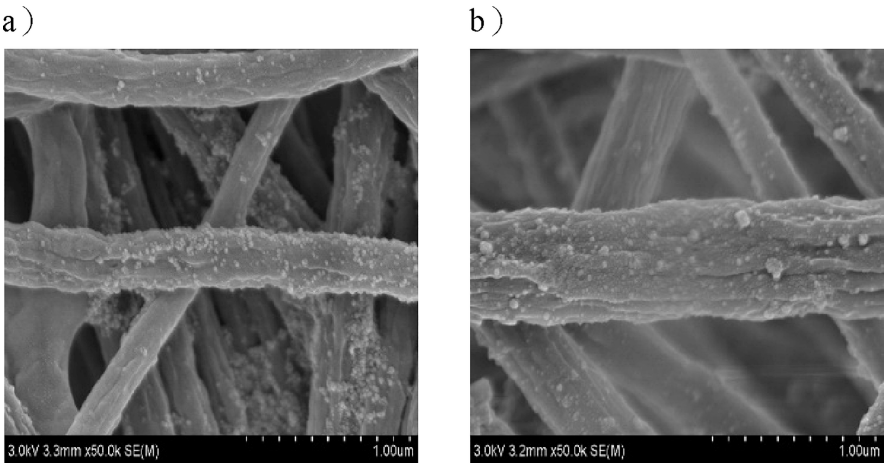

Figure 1. PAN/PVP nanofiber mat loaded with silver nanoparticles (a) after and (b) before tannic acid modification.

the solvent and PAN, a light yellow transparent spinning solution was obtained. Then, electrospinning was performed, and the corresponding parameters and operations were the same as those used for the preparation of the PAN/PVP nanofiber mat.

2.2.2. Modification of the PAN/PVP Nanofiber Mat. A 0.001 mol/L tannic acid solution was prepared, and the prepared electrospun nanofiber felt was immersed in the tannic acid solution for 0.5 h. Then, the nanofiber mat was removed from the tannic acid solution, washed three times with deionized water, and dried at 40 °C for subsequent processing.

2.2.3. Preparation of the PAN/PVP Nanofiber Mat Loaded with Silver Nanoparticles. Tollens' reagent was first prepared by slowly adding 0.02 mol/L ammonia to a beaker containing 0.02 mol/L silver nitrate. The beaker was shaken while the droplets were added until the color of the solution changed from brown turbidible to transparent and clear. Then, the treated PAN/PVP nanofiber mat was immersed in Tollens' reagent for 1 h to adsorb silver ammonia ions on the electrospun nanofiber mat as silver species for subsequent reduction reactions. Subsequently, 0.5 mol/L glutaraldehyde was added to the solution to achieve reduction, and the mixture was maintained at room temperature for 1 h in light. The membrane was removed, washed three times with distilled water, and dried in the oven at 40 °C. PAN/PVP nanofiber mats with different silver nanoparticle loadings were prepared by increasing the reduction time.

2.2.4. SERS Detection of Target Analytes. Before the detection of basic copper chloride, an analyte with a small molecular structure, simple SERS spectrum, and obvious characteristic peak (R6G) was selected to determine the SERS sensitivity of the PAN/PVP nanofiber mat loaded with silver nanoparticles.

In Raman detection, under the same conditions (laser power, objective magnification, acquisition time, etc.), different wavelengths of laser are selected for probe molecules, which results in different Raman signals. According to the law, the shorter the laser wavelength, the stronger is the Raman signal of the probe molecule. Therefore, a 532 nm-short wavelength laser is usually preferred. However, R6G as the probe molecule will have fluorescence effect under the action of the 532 nm laser, which interferes with the peak value in the range of 1200−1600 cm^{-1}, affecting the analysis of the R6G characteristic peak. Therefore, 785 nm with low fluorescence interference was selected as the detection laser wavelength for R6G.[34,35]

First, a series of aqueous solutions of R6G with concentrations of 10^{-1}, 10^{-3}, and 10^{-5} mol/L was prepared. Then, the prepared nanofiber felt was cut into small squares of 0.5 and 1 cm, and these squares were spread evenly on its surface after dropping 0.5 mL of R6G aqueous solution. The solution was dropped from the center of the prepared sample to gradually spread R6G aqueous solution over the entire surface of the sample. Then, the squares were dried in air. Finally, under a 50× objective lens, SERS spectra were collected with a 785 nm laser having a power of 5 mW. To avoid substrate damage, the laser intensity was set to 0.05%, the exposure time was 10 s, and the acquisition range was 100−2000 m^{-1}.

2.2.5. SERS Detection of Basic Copper Chloride. First, basic copper chloride was ground into powder and evenly spread on a paper. Then, the corner of the electrospinning nanofiber felt was held using tweezers and placed on the basic copper chloride powder for 3 s before it was removed. Afterward, the substrate with particles was flattened with a glass sheet, and the Raman test sample was prepared. The test settings are presented in Section 2.2.4. Finally, under the 50× objective lens, SERS spectra were collected with a 532 nm laser having a power of 5 mW. To avoid substrate damage, the laser intensity was set to 1%, the exposure time was 10 s, and the acquisition range was 100−3600 cm^{-1}.

3. RESULTS AND DISCUSSION

3.1. Effect of Tannic Acid on Silver Nanoparticle Stability. Tannic acid (TA) is a natural polyphenol with excellent properties, such as UV absorption, free radical scavenging, adhesion, reduction, antibacterial activity, and secondary reactivity.[9−12] In addition, TA can interact with various metal ions, and it has a six-member-ring chelator structure, which can rapidly nucleate silver atoms around the *o*-dihydroxy phenyl group of tannic acid under appropriate conditions.[13] Silver nanoparticles have been widely studied for the SERS effect. The small size and uniform density of silver nanoparticles on substrates are the keys to achieve multiple hot spots and high sensitivity. To explore the influence of tannins on the stability of silver nanoparticles, the contrast experiment was conducted. First, the PAN/PVP nanofiber mat was processed, and two parts were cut. The first part was modified

https://doi.org/10.1021/acsomega.2c06376
ACS Omega 2023, 8, 3091−3101

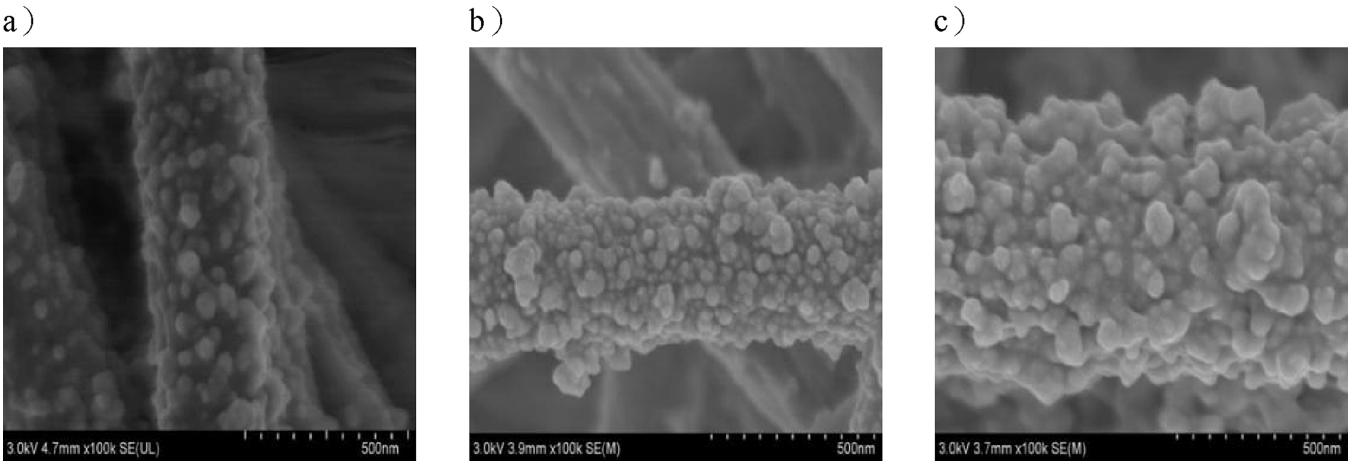

Figure 2. Morphology and structure of silver nanoparticles reduced (a) once, (b) twice, and (c) thrice using glutaraldehyde with the PAN/PVP nanofiber mat.

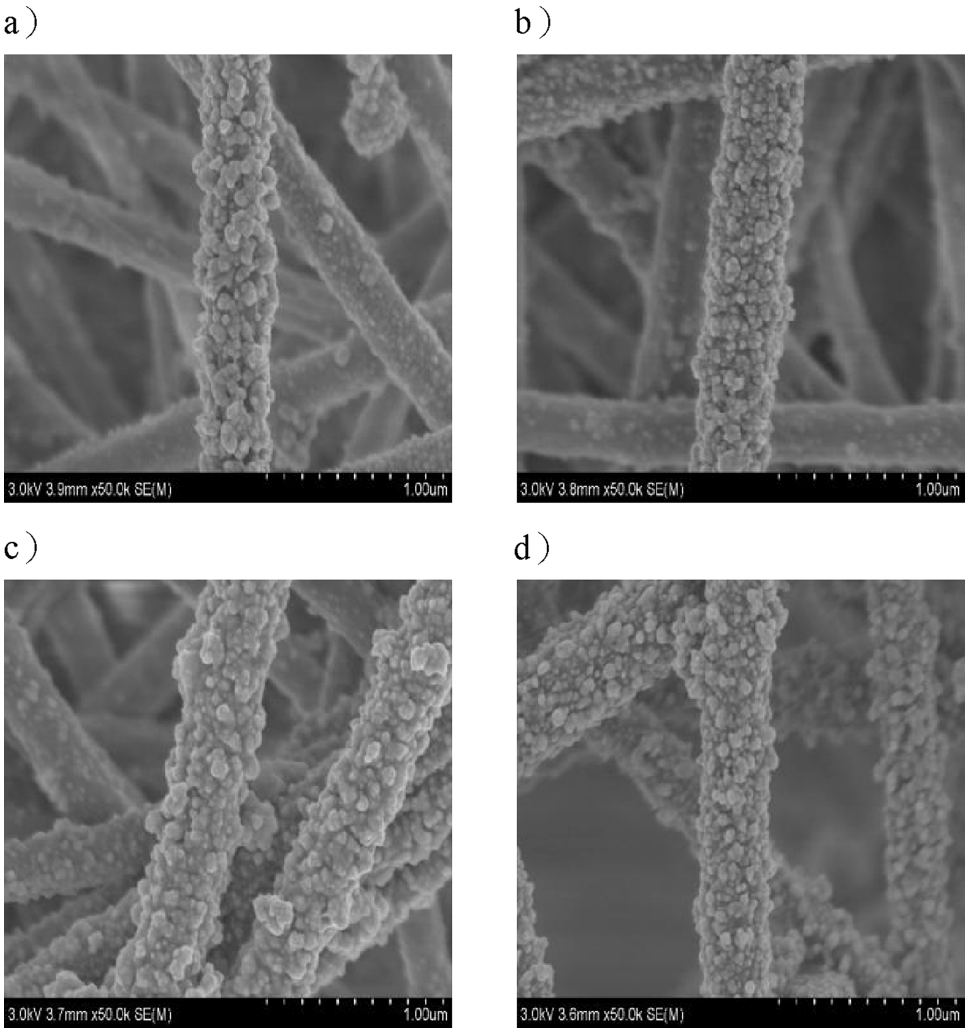

Figure 3. Reduction of silver nanoparticles by PAN/PVP nanofiber mat glutaraldehyde. (a) Reduced twice for 1 h; (b) reduced twice for 1.5 h; (c) reduced three times for 1 h; and (d) reduced three times.

with TA before being loaded with silver nanoparticles, and the other part was directly loaded with silver nanoparticles. After reduction, silver nanoparticles were washed with deionized water and dried in the oven. Silver nanoparticles were loaded and reduced only once. Figure 1 presents the field-emission SEM image of the corresponding PAN/PVP nanofiber mat loaded with silver nanoparticles under the aforementioned conditions. The number of silver nanoparticles loaded onto the modified nanofiber mat was high because TA makes the nanofiber show metal ion active carrier points, and thus, silver

https://doi.org/10.1021/acsomega.2c06376
ACS Omega 2023, 8, 3091−3101

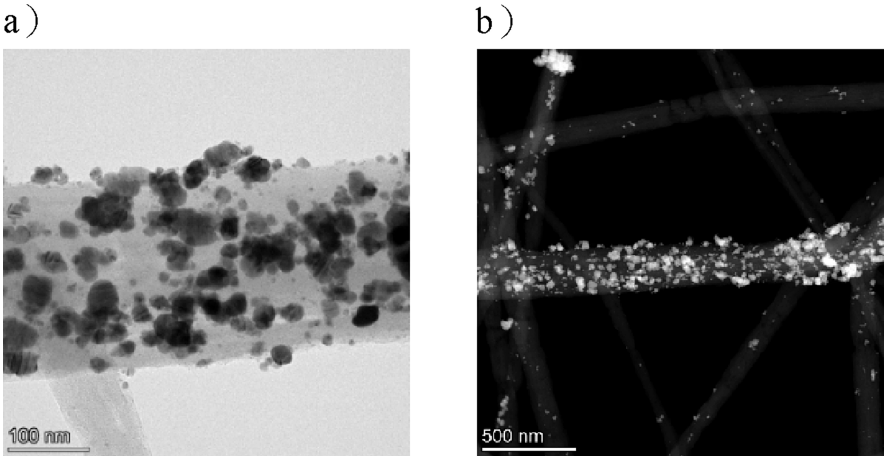

Figure 4. PAN/PVP silver nanofiber mat (after reduction for three times) (a) TEM; (b) HRTEM.

ions can easily grow uniformly on the nanofiber. The loading conditions of some large particles are presented in Figure 1b, which indicates that silver nanoparticles show partial aggregation phenomenon. Figure 1a shows an even distribution of silver nanoparticles.

After modification, the nanofiber reacts with silver ammonia solution for the first time, and a small amount of TA is dissolved in silver ammonia solution. After modification, most TA is used as the active site on the nanofiber to combine with the silver ammonia ion. Because TA has reducing properties and due to a very small amount of reduced silver ions, a small amount of silver nanoparticle loading can be observed on the surface of the nanofiber, and its size is about 10 nm.

As a polyphenolic macromolecule, TA contains a large number of phenolic hydroxyl groups and benzene rings, which can chelate with metal ions and proteins. As shown in Figure 6b, after TA modification and silver nanoparticle loading, the peak value at 3405 cm^{-1} becomes wider and weaker, which may be due to the phenolic hydroxyl group and the amino group that belongs to the tensile vibration of the Ar−OH group in tannic acid;[36] 2245 cm^{-1} belongs to the tensile vibration of the nitrile group, and the peak value appears at 3405 cm^{-1}, indicating that the PAN nitrile group is partially hydrolyzed to amide. The peak strength at 2245, 1659, and 1452 cm^{-1} was decreased. These results indicated that PAN/PVP nanofibers were successfully modified with TA.[37]

3.2. Effects on Silver Nanoparticle Morphology. Hot spots are defined as the junction or gaps between metal particles.[14] Although there is a hot spot effect among the agglomerated nanoparticles, the characteristics of the hot spot mainly depend on the shape and size of nanoparticles. Studies have shown that the optimal size range of silver nanoparticles for SERS is 20−70 nm.[14,15]

Therefore, the effect of reduction times on the morphology of silver nanoparticles was discussed. The concentration of Tollens' reagent and glutaraldehyde and other conditions were the same. The tannic acid-modified and washed and dried substrate was immersed in Tollens' reagent, and 0.5 mol/L glutaraldehyde was added to the silver ammonia solution for the reduction reaction. The PAN/PVP nanofiber mat loaded with silver nanoparticles was prepared with single, twice, and thrice reductions by changing the number of substrate immersion reduction times. Figure 2 shows the field-emission SEM images of the corresponding PAN/PVP nanofiber mat loaded with silver nanoparticles under the aforementioned conditions. When the reduction time was changed, the amount of silver nanoparticles attached to the nanofiber surface increased sharply. After three reductions, silver nanoparticles almost completely covered the nanofiber surface because silver nanoparticles could easily grow on the generated seeds. The silver nanoparticles were densely piled on the nanofibers after glutaraldehyde reduction. However, silver nanoparticles were mostly spherical, with the diameter of 20−50 nm, their growth diameter was stable because reduction was performed by adjusting the reduction times, and the same concentration of Tollens' reagent was employed for each reduction to maintain the concentration of silver ammonia ions in a certain range. After addition of glutaraldehyde, when silver ammonia ions diffused onto the nanofiber surface, the reduced, ellipsoidal silver nanoparticles with uniform particle size on the surface were obtained. The comparison between primary and tertiary reductions showed that with the increase in the reaction time, silver nanoparticles not only loaded on the nanofiber mat surface but also gradually penetrated the underlying nanofiber.

3.3. Effect of the Reduction Time on Silver Nanoparticles. To determine the effect of the reduction time on the experiment, the two different loadings of silver nanoparticles on the PAN/PVP nanofiber mat were studied after the addition of the reducing agent at 1 and 1.5 h. Figure 3 shows the field-emission SEM images of the corresponding PAN/PVP nanofiber mat loaded with silver nanoparticles under the aforementioned conditions. Silver nanoparticles loaded on the nanofiber surface increased with the increase in the reaction time.

The comparison between the reduction times of 1 and 1.5 h showed that the diameter of the particles loaded onto nanofibers increased after 1.5 h of reduction, and the diameter was 50−100 nm because as the reduction reaction progressed, the amount of silver ammonia ions decreased in the solution. Unreduced silver ammonia ions continued to react, and silver nanoparticles were highly likely to grow on the generated seeds, which resulted in the formation of larger particles.

3.3.1. TEM Morphology Characterization of the PAN/PVP Nanofiber Mat. The PAN/PVP silver nanosubstrate was characterized using TEM and HRTEM to study the morphology of the nanofiber mat at the microscopic scale. The treatment of nanomaterials included the use of deionized water as solvent and observation of the morphological characteristics of nanofibers after dispersion in the aqueous solution through ultrasound. Some nanoparticles were lost in

https://doi.org/10.1021/acsomega.2c06376
ACS Omega 2023, 8, 3091−3101

this method. Figure 4a,b shows the TEM and HRTEM images, respectively, of the substrate that was reduced three times. Silver nanoparticles were adsorbed onto the nanofibers, and the particle size was 20−50 nm. No obvious aggregation phenomenon was observed.

3.4. Crystal Structure of the PAN/PVP Nanofiber Mat. The crystal structure of the PAN/PVP silver nanofiber mat was further analyzed through XRD. According to the comparison with PAN diffraction standard cards, 29.3° is the diffraction peak of PAN. When PVP was introduced, this peak segment was gradually shifted to a small angle. According to the calculation, this phenomenon occurred because PVP introduction led to adverse PAN crystallization[15,16] (curve a in Figure 5). On the substrate loaded with silver nanoparticles,

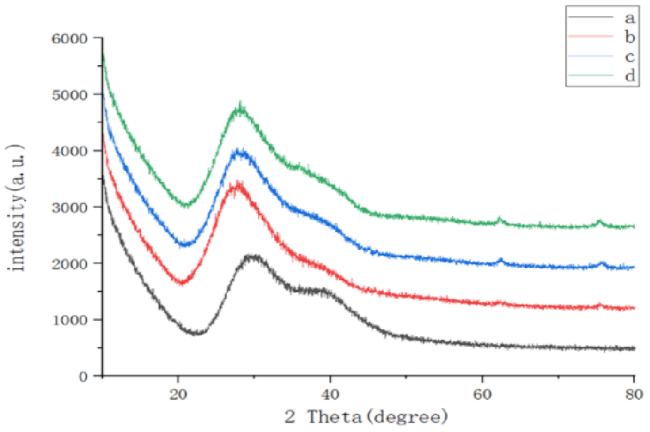

Figure 5. PAN/PVP silver nanofiber felt XRD (a) blank substrate; (b) PAN silver nanosubstrate (reduced once); (c) PAN silver nanosubstrate (reduced twice); and (d) PAN silver nanosubstrate (reduced three times).

the diffraction peak seen at 29.3° started to shift slightly, indicating an increase in the lattice constant, suggesting that atoms larger than the main atomic radius were incorporated. The peak at 40° was attributed to the plane reflection of the carbon structure in PAN. In addition, spikes appeared at 62.5 and 75.5°, which corresponded to the (220) and (311) of the face-centered cubic Ag crystal (JCPDF, No.04−0783),[17] and no other diffraction peaks were obtained, which indicated that the loading of pure Ag nanoparticles provided certain chemical stability. The peak intensity increased with the increase in the reduction time, indicating that silver nanoparticles gradually increased. As the reduction reaction proceeds, the amount of silver nanoparticles increases and the peak value gradually weakens, which also indicate that the silver nanoparticles tend to wrap the nanofiber mat.

3.5. Infrared Characterization of the PAN/PVP Nanofiber Mat. To analyze the interactions among the PAN/PVP nanofiber mat, basic copper chloride, and silver nanoparticles, infrared characterization was performed on blank substrates, substrates supplemented with the basic copper chloride powder, and substrates loaded with silver nanoparticles. Figure 6a shows the comparison between the blank substrate and basic copper chloride powder. The peak seen at 2243 cm^{-1} is attributed to C≡N tensile vibration, and that at 1440 cm^{-1} corresponds to C−H in-plane deformation vibration, which belongs to the characteristic peak of PAN. The peak obtained at 1659 cm^{-1} is attributed to C−O stretching vibration, and those at 1494 and 1289 cm^{-1} are attributed to C═C and C−N stretching vibrations, respectively, which belong to the characteristic peaks of PVP. This indicated that the interaction between the two polymers was poor, and the interaction between PAN and PVP macromolecules in nanofibers was weak.

Figure 6b shows the comparison between the blank substrate and loaded silver nanoparticles. The infrared band of C−N showed blue shift (1289 to 1263 cm^{-1}) because the coordination between N and silver in PVP had a spatial effect, with N having lower electronegativity and higher electron-donating capacity than O. Space effect was not the main factor affecting PVP. Therefore, Ag and PVP interacted mainly through the coordination between N and silver ions. Two new peaks appeared at 1027 and 800 cm^{-1} due to the coordination of N atoms in Ag and PAN, and the band shifts from 1224 to 1169 cm^{-1} and from 1494 to 1452 cm^{-1} were observed. PVP and PAN exhibited valence bonds that could bind to silver nanoparticles. PVP interacted with silver nanoparticles through amide bonds, and PAN interacted with silver nanoparticles through the amino group. Figure 6b shows the comparison of the infrared spectra of PAN/PVP nanofibers loaded with and for silver nanoparticles; as shown, the fiber mat containing silver nanoparticles has a peak value at 1035 cm^{-1}, which is related to the N−C−O group, and the peak at 800 cm^{-1} denotes the vibration of the pyrrolidone ring.[38] In addition, a part of the wave number band disappeared between 800 and 1500 cm^{-1}, which also indicated that Ag nanoparticles were densely embedded on the nanofiber mat.

To explore the action mode of basic copper chloride powder on the substrate, the PAN/PVP silver nanofiber mat loaded with basic copper chloride powder was characterized by Raman spectra and compared with a curve. The infrared spectra of 3441 and 3433 cm^{-1} corresponding to the Raman spectra were as ascribed to the stretching vibrations of the hydroxyl group. The spectra seen at 925/865/833/740 cm^{-1} were attributed to the deformation modes of Cu−O−H (δCu−O−H). Compared with the infrared spectrum of standard basic copper chloride (865/79/785/700 cm^{-1}), a red shift was observed in the Raman spectra; 118 is defined as the Cu tensile vibration (δO−Cu), and 138 is attributed to Cu−Cl tensile vibration. The interaction of basic copper chloride molecules with the substrate was related to O−Cu.[16,28−30]

3.6. TG-DTA Characterization of the PAN/PVP Nanofiber Mat. At approximately 300 °C, PAN cyclization produced considerable exothermic heat, whereas at 600 °C, PVP decomposition exothermic heat was generated[16,26−28] (Figure 7c). The addition of PVP affected PAN cyclization, and the peak was not obvious at approximately 300 °C (Figure 7a). The TG curve of the blank substrate showed a tendency to decelerate decomposition at 300−500 °C. This phenomenon may be attributed to the high surface energy of nanoparticles, which could reduce the surface area through aggregation and coalescence. In addition, physical desorption of the capping agent (PVP) of silver nanoparticles was observed at 30−150 °C, and no such phenomenon was found in characterization, suggesting that PVP did not lead to a coating effect on silver nanoparticles.

3.7. Study on the SERS Performance of the PAN/PVP Nanofiber Mat. *3.7.1. R6G as a Probe Molecule.* Figure 8a shows the Raman spectra of different concentrations of R6G (as probe molecules) and PAN/PVP silver nanoparticles as SERS substrates. When PAN/PVP silver nanoparticles were used as the SERS substrate, almost all the Raman characteristic

https://doi.org/10.1021/acsomega.2c06376
ACS Omega 2023, 8, 3091−3101

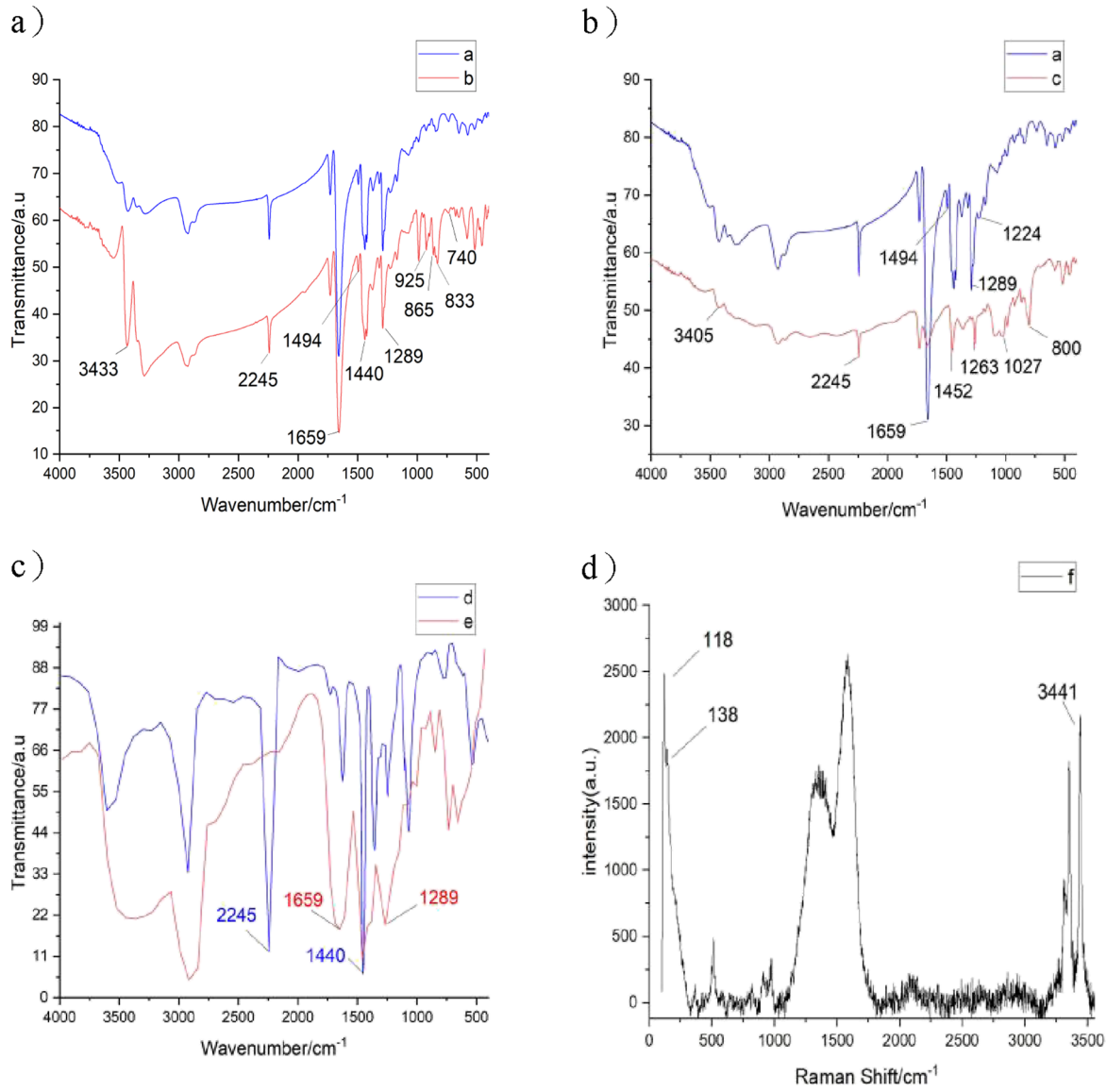

Figure 6. Infrared spectra of PAN/PVP nanofiber mats, (a): (curve a) PAN/PVP blank substrate; (curve b) PAN/PVP blank substrate + alkaline copper chloride powder. (b): (curve a) PAN/PVP blank substrate; (curve c) PAN/PVP blank substrate + silver nanoparticles. (c): (curve d) PAN blank substrate; (curve e) PVP blank substrate. Raman spectrogram, (d): (curve f) PAN/PVP silver nanofiber mat (reduced once) + basic copper chloride powder.

peaks of R6G could be identified. The comparison results showed that when R6G was directly applied for Raman detection (dropping R6G on the PAN/PVP fiber mat without the silver nanosubstrate), the characteristic peak was not obvious (Figure 8a, curve a). For the PAN/PVP silver nanosubstrate, with the increase in the R6G concentration, the peak value became more prominent after Raman enhancement, where the peaks at 1575 and 1088 cm^{-1} were mainly attributed to the benzene torus in-plane vibration, those at 1511, 1127, 774, and 608 cm^{-1} were attributed to the R6G oxanthracene ring in-plane vibration, and those 1362 and 614 cm^{-1} were assigned to the C−C plane bending vibration and C−C−C torus vibration, respectively.[18−20]

To explore the effects of PVP on SERS of the nanofiber felt, experiments were conducted using R6G as the probe molecule and the PAN silver nanofiber felt as the SERS substrate. Figure 8b shows the Raman spectrograms with different concentrations of R6G as probe molecules and the PAN silver nanofiber mat as SERS substrates. The results indicated that partial obvious characteristic peaks of R6G appeared at 0.1 mol/L, and the characteristic peaks of benzene torus and oxanthracene ring could not be seen. These results indicated that for PVP used as a stabilizer, the reduced silver nanoparticles were maintained in a certain size range, which effectively prevented the aggregation of silver nanoparticles.[21−23] Maintaining silver nanoparticles within a certain size range is crucial for hotspot formation.

To investigate the effect of nanofibers on silver nanoparticles, PAN and PVP nanofiber blankets were prepared, both of which were modified by TA before reducing silver nanoparticles three times. Then, the SERS effect of 10^{-1} mol/L R6G was determined. Figure 8c shows the results of Raman data. By comparing the two, it was found that silver nanoparticles exerted a certain SERS effect on the two nanofiber mat, and the peak was enhanced. However, certain

https://doi.org/10.1021/acsomega.2c06376
ACS Omega 2023, 8, 3091−3101

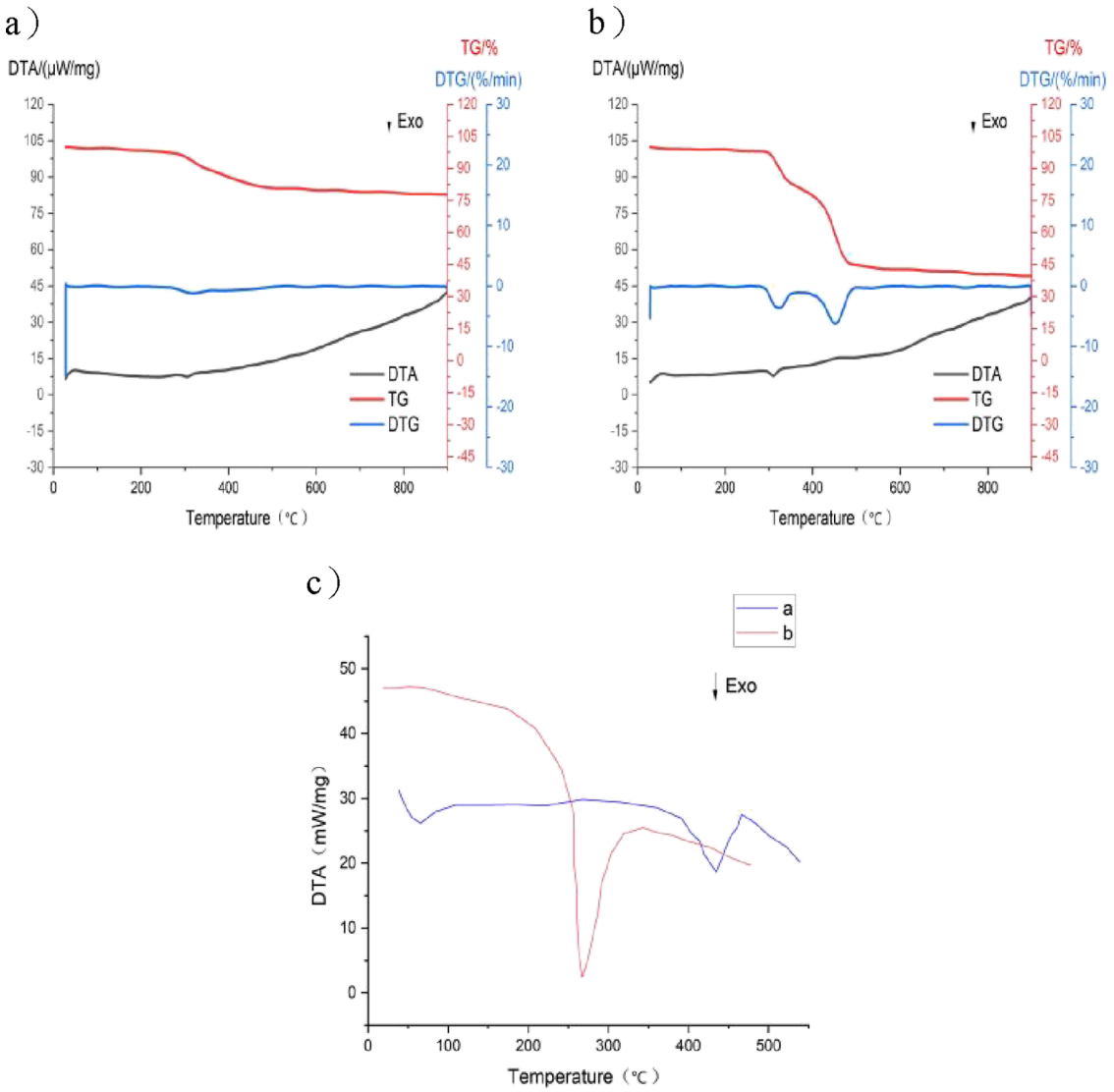

Figure 7. TG-DTA diagram of the PAN/PVP nanofiber mat, (a) PAN/PVP blank substrate, (b) PAN/PVP silver nanofiber mat, and (c) DTA diagram of the PAN and PVP, curve a: PAN nanofiber mat; curve b: PVP nanofiber mat.

incomplete characteristic peaks were observed, which may be attributed to the aggregation of silver nanoparticles.

3.7.2. Basic Copper Chloride as the Probe Molecule. To simulate the surface of the bronze relics, the influence of SERS on nanofibers was studied by using basic copper chloride as the corrosion component on the bronze relic surface. Figure 9 shows the Raman spectra of the loaded silver nanoparticles with different amounts of basic copper chloride as the probe molecule and PAN/PVP silver nanoparticles as the SERS substrate. The standard Raman peaks of $Cu_2(OH)_3Cl$ were observed at 122, 360, 513, 846, 911, 974, 3329, 3349, and 3433 cm^{-1}. The characteristic peak of the PAN/PVP nanofiber mat without silver nanoparticles was not obvious in the Raman spectrum. After loading silver nanoparticles, the characteristic peak of basic copper chloride was identified. However, on the PAN/PVP nanofiber mat with different amounts of silver nanoparticles reduced, the characteristics of the SERS effect did not enhance because the size of silver nanoparticles was uniform, and the number of silver nanoparticles increased. In the second and third reductions, the SERS effect was almost the same, possibly due to the detection of the basic copper chloride powder.

Two broad overlapping peaks appeared in the Raman spectra at 1050−1700 cm^{-1}, which were attributed to the PAN carbon peaks. The peak at 1590 cm^{-1} corresponding to the stretching vibration of carbon−carbon double bonds and carbon−nitrogen double bonds of polycyclic aromatic hydrocarbons and that at 1360 cm^{-1} resulted from carbon (graphite) mixed with SP2 and SP3.[24] The carbon peaks of PAN are represented on the Raman spectra of R6G and basic copper chloride as probe molecules. The experimental results showed that the influence of the characteristic peaks on PAN molecules was small, and the characteristic peaks of probe molecules could be seen.

3.7.3. Enhancement Factor (EF) Calculation. Generally, the performance of surface Raman reinforced substrates is evaluated by calculating the enhancement factor (EF).[31] To explore and quantify the SERS effect of the substrate, R6G was used as the probe molecule, and the intensity of Raman peak located at 1511 cm^{-1} was used. The PAN/PVP silver nanofiber mat with 10^{-5} mol/L R6G aqueous solution was used as the

https://doi.org/10.1021/acsomega.2c06376
ACS Omega 2023, 8, 3091−3101

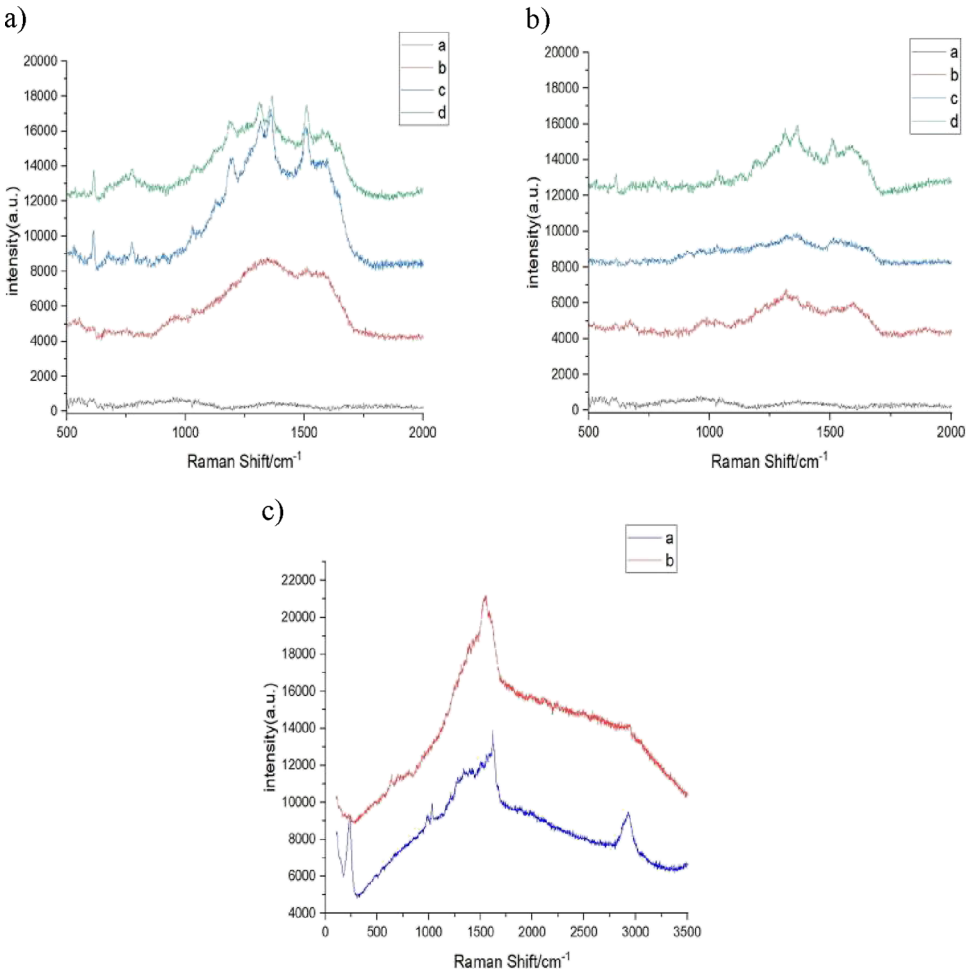

Figure 8. (a) Raman spectra of the PAN/PVP nanofiber mat with different concentrations of R6G as probe molecules. Unloaded silver nanoparticles: curve a: 10^{-1} mol/L; silver nanoparticles loaded: curve b: 10^{-1} mol/L, curve c: 10^{-3} mol/L, curve d: 10^{-5} mol/L. (b) Raman spectra of the PAN nanofiber mat with different concentrations of R6G as probe molecules. Unloaded silver nanoparticles: curve a: 10^{-1} mol/L; silver nanoparticles loaded: curve b: 10^{-1} mol/L, curve c: 10^{-3} mol/L, and curve d: 10^{-5} mol/L. (c) Raman spectra of the nanofiber mat with 10^{-1} mol/L R6G. Silver nanoparticles loaded: curve a: PAN nanofiber mat; curve b: PVP nanofiber mat.

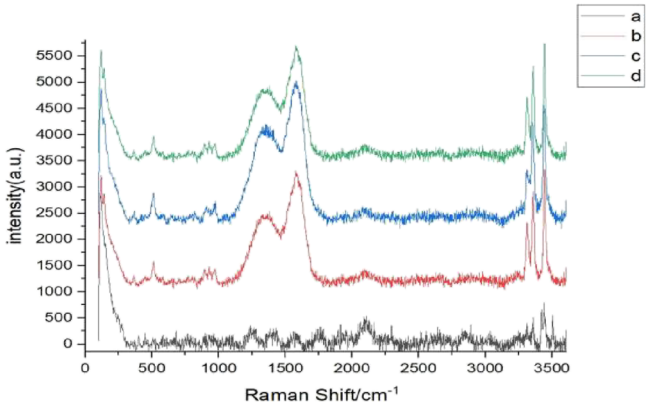

Figure 9. Raman spectra of the PAN/PVP nanofiber mat with basic copper chloride as the probe molecule. Unloaded silver nanoparticles: curve a: silver nanoparticles loade;: curve b: reduced once; curve c: reduced twice; and curve d: reduced three times.

SERS substrate. EF was calculated according to the following formula:[25]

$$EF = (I_{SERS}/I_{bulk}) \times (N_{bulk}/N_{SERS})$$

where I_{SERS} and I_{bulk} are the peak intensities of the same wave number in SERS and standard Raman spectra of the detected molecule and N_{SERS} and N_{bulk} are the number of molecules detected in SERS and standard Raman spectra of the detected molecule, respectively. During the experiment, 0.1 mL of 10^{-1} mol/L aqueous solution of R6G was dispersed on the PAN/PVP nanofiber mat to characterize the standard Raman spectra. By dispersing 0.05 mL of 10^{-5} mol/L aqueous solution of R6G on the PAN/PVP silver nanofiber mat to characterize SERS, the ratio of N_{SERS} to N_{bulk} in the same laser spot area could be obtained. From Raman spectra, I_{SERS}/I_{bulk} was approximately 0.026; thus, EF was approximately 7.7×10.[6] EF calculation showed that the SERS substrate was effective for trace detection.

4. CONCLUSIONS

In this study, we developed a PAN/PVP silver nanofiber mat as the SERS substrate for trace detection. The morphology and structure of the prepared nanofiber mat were characterized through SEM and XRD. Uniform spherical silver nanoparticles could be obtained on the nanofibers at the deposition time of 1.5 h in Tollens' reagent and reduction thrice with glutaraldehyde as the reducing agent. R6G was selected to

https://doi.org/10.1021/acsomega.2c06376
ACS Omega 2023, 8, 3091−3101

evaluate the SERS performance of the substrate, and the results showed that the SERS sensitivity of the PAN/PVP silver nanofiber mat was extremely high. The use of basic copper chloride as the probe molecule to simulate the surface composition of ancient bronze ware also showed the high SERS sensitivity of the nanofiber mat, which can be used for the trace analysis of the surface composition of the bronze cultural relics.

AUTHOR INFORMATION

Corresponding Author

Xia Huang − *School of Materials Science and Engineering, Zhengzhou University, Zhengzhou, Henan 450001, P.R. China*; Phone: +86- 371- 67781590; Email: happyhxia@163.com; Fax: +86-371-67781590

Authors

Pengyang Li − *School of Chemical Engineering, Zhengzhou University, Zhengzhou, Henan 450001, P.R. China*; orcid.org/0000-0003-4793-6079

Yahui Zhang − *School of Materials Science and Engineering, Zhengzhou University, Zhengzhou, Henan 450001, P.R. China*

Junying Chen − *School of Chemical Engineering, Zhengzhou University, Zhengzhou, Henan 450001, P.R. China*; orcid.org/0000-0003-1325-9663

Jiachang Chen − *Henan Provincial Institute of Cultural Relics and Archaeology, Zhengzhou, Henan 450000, P.R. China*

Lei Li − *PLA Strategic Support Force Information Engineering University Henan Key Laboratory of Imaging and Intelligent Processing, Zhengzhou, Henan 450002, P.R. China*

Xiaoqi Xi − *PLA Strategic Support Force Information Engineering University Henan Key Laboratory of Imaging and Intelligent Processing, Zhengzhou, Henan 450002, P.R. China*

Complete contact information is available at: https://pubs.acs.org/10.1021/acsomega.2c06376

Notes

The authors declare no competing financial interest.

ACKNOWLEDGMENTS

We are grateful for the financial support of The National Key Research and Development Program of China (no. 2020YFC1522000) for funding this work.

REFERENCES

(1) An, M.; Li, X. Theoretical study on the interaction between thiazoles and powdery rust on the surface of bronze ware. *J. Mol. Sci. (Int. Ed.)* **2014**, *30*, 410−415.

(2) Liao, Y. Protection of Cultural relics such as Western Zhou Dynasty Bronze Kettle, Western Han Dynasty Five-Baht Coin and Sui Dynasty Bronze Mirror. *J. Northwest Univ., Nat. Sci, Ed* **2003**, *01*, 45−48.

(3) Philippe, C.; Aurélie, T.; Michel, M.; Philippe, M. On-site Raman and XRF analysis of Japanese/Chinese bronze/brass patina−the search for specific Raman signatures. *J. Raman Spectrosc.* **2012**, *43*, 799−808.

(4) Liu, W.; Du, J.; Jing, C. Research progress of surface enhanced Raman spectroscopy in the detection of environmental pollutants. *Environ. Chem.* **2014**, *33*, 217−228.

(5) Sun, Y.; Shi, L.; Mi, L.; Guo, R.; Li, T. Recent progress of SERS optical nanosensors for miRNA analysis. *J. Mater. Chem. B* **2020**, *B8*, 5178−5183.

(6) Hong, Z. Q.; Zhang, Y. P.; Lu, J.; He, D. Research progress of surface enhanced Raman scattering substrates and mechanism. *Nonferrous Met. Mater. Eng.* **2017**, *38*, 119−122.

(7) Lee, J.; Min, K.; Kim, Y.; Yu, H. K. Surface-enhanced raman spectroscopy (SERS) study using oblique angle deposition of Ag using different substrates. *Materials* **2019**, DOI: 10.3390/ma12101581.

(8) Yan, Y.; Zhijie, Z.; Menghui, W.; Zhihui, W.; Yanbao, Z.; Lei, S. Highly sensitive surface-enhanced Raman Spectroscopy Substrates of Ag@ PAN electrospinning nanofibrous membranes for direct detection of bacteria. *ACS Omega* **2020**, *5*, 19834−19843.

(9) Sharma, B.; Frontiera, R. R.; Henry, A. I.; Ringe, E.; Van Duyne, R. P. SERS: Materials, applications, and the future. *Mater. Today* **2012**, *15*, 16−25.

(10) Jiankang, C.; Qi, J.; Zi, C.; Xue, J.; Li, J.; Xiaoyin, L. Research progress of electrospinning polyacrylonitrile fiber and its application in electrochemical supercapacitor. *J. Funct. Mater.* **2017**, *48*, 2026−2032.

(11) Wentao, Y.; Mengqi, S.; Chenxi, D.; Lifen, L.; Congjie, G. Applications of tannic acid in membrane technologies: A review. *Adv. Colloid Interface Sci.* **2020**, *264*, No. 102267.

(12) Mesgarzadeh, I.; Akbarzadeh, A. R.; Rahimi, R.; Ali, M. Novel design, preparation, characterization and antimicrobial activity of silver nanoparticles during oak acorns bark retrograde. *Z. Phys. Chem.* **2018**, *232*, 209−221.

(13) Ham, X.; Weipin, H.; Kefeng, R.; Yimin, T. Spraying layer-by-layer assembly of tannin-Fe^{3+} and polyethyleneimine for antibacterial coating. *Colloid Interface Sci. Commun.* **2021**, *42*, No. 100422.

(14) Tao, C.; Hong, W.; Gang, C.; Yong, W.; Yuhua, F.; Wei, S. T.; Tom, W.; Hongyu, C. Hotspot-induced transformation of surface-enhanced Raman scattering fingerprints. *ACS Nano* **2010**, *4*, 3087−3094.

(15) Han, R.; Meilin, Y.; Fu, Y. Z.Preparation and properties of ultrafine PAN/PVP composite nanofibers. *New Chem. Mater.***2015**, *43* () 89−95.

(16) Zhang, Z.; Li, X.; Wang, C.; Fu, S.; Liu, Y.; Shao, C. Polyacrylonitrile and carbon nanofibers with controllable nanoporous structures by electrospinning. *Macromol. Mater. Eng.* **2009**, *294*, 673−678.

(17) Purbia, R.; Nayak, P. D.; Paria, S. Visible light-induced Ag nanoparticle deposited urchin-like structures for enhanced SERS application. *Nanoscale* **2018**, *10*, 12970−12974.

(18) Yang, K. H.; Liu, Y. C.; Yu, C. C. Simple strategy to improve surface-enhanced Raman scattering based on electrochemically prepared roughened silver substrates. *Langmuir* **2010**, *26*, 11512−11517.

(19) Chanjuan, C.; Cheng, Z.; Guokun, L.; Bin, R. Electrochemical surface enhanced Raman spectroscopy of rhodamine 6G on silver surface. *Electrochemistry* **2016**, *22*, 32−36.

(20) Pan, J.; Li, M.; Luo, Y. Y.; Wu, H.; Zhong, L.; Wang, Q.; Li, G. H. Synthesis and SERS activity of V2O5 nanoparticles. *Appl. Surf. Sci.* **2015**, *333*, 34−38.

(21) Jin, W. J.; Lee, H. K.; Jeong, E. H.; Park, W. H.; Youk, J. H. Preparation of polymer nanofibers containing silver nanoparticles by using poly (N-vinylpyrrolidone). *Macromol. Rapid Commun.* **2005**, *26*, 1903−1907.

(22) Eisa, W. H.; Abdel-Moneam, Y. K.; Shabaka, A. A. M.; Abd ElHameed, M. H. In situ approach induced growth of highly monodispersed Ag nanoparticles within free standing PVA/PVP films. *Spectrochim. Acta, Part A* **2012**, *95*, 341−346.

(23) Xin, Q.; Tonnam, B.; Ya, Z.; Kristen, A. How structure-directing agents control nanocrystal shape: polyvinylpyrrolidone-mediated growth of Ag nanocubes. *Nano Lett.* **2015**, *15*, 7711−7717.

(24) Sutasinpromprae, J.; Jitjaicham, S.; Nithitanakul, M.; Meechaisue, C.; Supaphol, P. Preparation and characterization of ultrafine electrospun polyacrylonitrile fibers and their subsequent pyrolysis to carbon fibers. *Polym. Int.* **2006**, *55*, 825−833.

(25) ÁlvarezPuebla, R. A. Effects of the Excitation Wavelength on the SERS Spectrum. *J. Phys. Chem. Lett.* **2012**, *3*, 857−866.

(26) Chen, Z. M.; Chen, J. F.; Xue, F. F.; Qun, X. Silver mirror reaction on the surface of silica microspheres infiltrated by silver ammonia solution. *World Sci-Tech R & D* **2008**, *04*, 387−390.
(27) Bao, T. T.; Kim, Y.; Lee, J.; Lee, J. G. Preparation and thermal analysis of Sn-Ag nano solders. *Mater. Trans.* **2010**, 2145.
(28) Li, S.; Liu, P.; Wang, Q. Study on the effect of surface modifier on self-aggregation behavior of Ag nano-particle. *Appl. Surf. Sci.* **2012**, *263*, 613−618.
(29) Wang, H.; Qiao, X.; Chen, J.; Wang, X.; Ding, S. Mechanisms of PVP in the preparation of silver nanoparticles. *Mater. Chem. Phys.* **2005**, *94*, 449−453.
(30) Zhao, Y.; Cui, H.; Zhang, J.; Ma, Y.; Tian, H.; Wu, L.; Cui, Q.; Ma, Y. Pressure-induced phase transformation of botallackite α-$Cu_2(OH)_3Cl$ with a two-dimensional layered structure synthesized via a hydrothermal strategy. *J. Phys. Chem. C* **2020**, *124*, 9581−9590.
(31) Wei, H.; McCarthy, A.; Song, J.; Zhou, W.; Vikesland, P. J. Quantitative SERS by hot spot normalization−surface enhanced Rayleigh band intensity as an alternative evaluation parameter for SERS substrate performance. *Faraday Discuss.* **2017**, *205*, 491−504.
(32) Jaworska, A.; Wojcik, T.; Malek, K.; Kwolek, U.; Kepczynski, M.; Ansary, A. A.; Chlopicki, S.; Baranska, M. Rhodamine 6G conjugated to gold nanoparticles as labels for both SERS and fluorescence studies on live endothelial cells. *Microchim. Acta* **2015**, *182*, 119−127.
(33) Gettens, R. J. Mineral alteration products on ancient metal objects. *Stud. Conserv* **1961**, *6*, 89−92.
(34) Dai, H.; Sun, Y.; Ni, P.; Lu, W.; Jiang, S.; Wang, Y.; Li, Z.; Li, Z. Three-dimensional TiO2 supported silver nanoparticles as sensitive and UV-cleanable substrate for surface enhanced Raman scattering. *Sens. Actuators, B* **2017**, *242*, 260−268.
(35) T, W. Y.Design and preparation of noble metal micro-nano Structures and their SERS properties, Ph. D. Dissertation, University of Science and Technology of China, PA, 2014.
(36) Jianlong, G.; Dingding, Z.; Qing, J.; Jianyong, Y.; Bin, D. Biomimetic and superwettable nanofibrous skins for highly efficient separation of oil-in-water emulsions. *Adv. Funct* **2018**, DOI: 10.1002/adfm.201705051.
(37) Jing, Z.; Chao-Hua, X.; Hong-Rui, M.; Ya-Ru, D.; Shun-Tian, J. Fabrication of PAN electrospun nanofibers modified by tannin for effective removal of trace Cr (III) in organic complex from wastewater. *Polymer* **2020**, DOI: 10.3390/polym12010210.
(38) Mikhail, K.; Alexander, L.; Daniela, G.; Aleksandr, M.; Giovanni, D. F. Ag/PVP/PAN nanocomposites with triangular nanoprisms of silver synthesized by UV-induced polymerization: Morphology manipulation and optical properties tuning. *Opt. Mater.* **2020**, No. 109746.
(39) Denis, P.; Siliu, T.; Melek, E.; Henry, D.; Svetlana, S. In situ SERS study of Rhodamine 6G adsorbed on individually immobilized Ag nanoparticles. *J. Raman Spectrosc..* **2006**, *37*, 762−770.

https://doi.org/10.1021/acsomega.2c06376
ACS Omega 2023, 8, 3091−3101